

Intensity of Raman modes as a temperature gauge in fluid hydrogen and deuterium

Cite as: J. Appl. Phys. **125**, 025901 (2019); <https://doi.org/10.1063/1.5070113>

Submitted: 19 October 2018 . Accepted: 16 December 2018 . Published Online: 09 January 2019

Miriam Peña-Alvarez, Philip Dalladay-Simpson, Xiao-Di Liu, Veronika Afonina, Hui-Chao Zhang, Ross T. Howie, and Eugene Gregoryanz



View Online



Export Citation



CrossMark

ARTICLES YOU MAY BE INTERESTED IN

Synthesis and stability of hydrogen selenide compounds at high pressure

The Journal of Chemical Physics **147**, 184303 (2017); <https://doi.org/10.1063/1.5004242>

Pressure-induced structural change and nucleation in liquid aluminum

Journal of Applied Physics **124**, 225903 (2018); <https://doi.org/10.1063/1.5054293>

In situ X-ray imaging of heterogeneity in dynamic compaction of granular media

Journal of Applied Physics **125**, 025902 (2019); <https://doi.org/10.1063/1.5057713>

Ultra High Performance SDD Detectors



AMETEK[®]
MATERIALS ANALYSIS DIVISION



See all our XRF Solutions

Intensity of Raman modes as a temperature gauge in fluid hydrogen and deuterium

HPSTAR
689-2019

Cite as: J. Appl. Phys. 125, 025901 (2019); doi: 10.1063/1.5070113

Submitted: 19 October 2018 · Accepted: 16 December 2018 ·

Published Online: 9 January 2019



Miriam Peña-Alvarez,¹ Philip Dalladay-Simpson,^{2,a)} Xiao-Di Liu,³ Veronika Afonina,¹ Hui-Chao Zhang,³ Ross T. Howie,² and Eugene Gregoryanz^{1,2,3,b)}

AFFILIATIONS

¹Centre for Science at Extreme Conditions and School of Physics and Astronomy, University of Edinburgh, Edinburgh, United Kingdom

²Center for High Pressure Science and Technology Advanced Research, Shanghai, China

³Key Laboratory of Materials Physics, Institute of Solid State Physics, CAS, Hefei, China

^{a)}philip.dalladay-simpson@hpstar.ac.cn

^{b)}e.gregoryanz@ed.ac.uk

ABSTRACT

The Raman spectra of liquid H₂(D₂) have been collected in diamond anvil cell as a function of temperature at 3 GPa covering the range from 80 to \sim 1000 K. Temperatures were measured using two independent methods: by thermocouple and from the relative intensity ratio of the present Raman modes. We find excellent agreement between the two methods in the low temperature regime (80 to 400 K) but observe discrepancies between these approaches at temperatures above 400 K. We attribute that the temperature difference between the two methods arises primarily from the proximity of the thermocouple relative to the heating elements and sample. Although not always available in high-pressure experiments, the metrology based on *in situ* physical properties of the sample is absolute and more reliable than the secondary gauges based on external devices.

Published under license by AIP Publishing. <https://doi.org/10.1063/1.5070113>

I. INTRODUCTION

Being the universe's most abundant element, hydrogen exists at conditions ranging from near-zero degrees in the vacuum of space to the extreme temperatures and pressures found in the interior of planets and stars. Although the pressure-temperature (P-T) values that mimic those deep below the surface of planets cannot be readily achieved in the experimental laboratory, comprehensive studies on hydrogen at lower pressures and temperatures provide valuable information which can be further extrapolated to gain insight into more extreme conditions.^{1–4} Over the past few years, technological advances have led to more than a twofold increase in the range of experimentally accessible pressures and temperatures in the hydrogen's phase diagram.^{5–10} As the P-T space is extended, an effort must be made for the continued development of pressure-temperature metrology.

In general, pressure measurements are based on established markers, such as ruby fluorescence for optical studies

or noble metal P-V equation of state for x-ray diffraction measurements.^{11,12} However, in diamond anvil cell (DAC) experiments that require pressures in excess of 100 GPa, diminished sample sizes rule out these conventional approaches, and the calibrated shift of the stressed edge of the diamond T_{2g} Raman mode (DE) is used to estimate pressures.^{13,14} Although widely adopted, the reproducibility of this method has been questioned, as it appears the shift of the DE is dependent on sample and anvil geometry. This is exemplified in room temperature compression experiments of hydrogen, where multiple studies have claimed the same phase transitions, but at different pressures.^{5,6} It was subsequently proposed that DE can give an estimate of pressure, but comparisons between studies should be cross-referenced through a physical property of the sample. In the case of hydrogen studies, the frequency of the intramolecular vibrational mode provides a valid standard for comparison.¹⁵ This self-consistent method for measuring pressure has been

adopted in isobaric low/high-temperature DAC studies of H₂ and D₂ above 100 GPa.^{9,15,16}

Accurately measuring temperature also presents a challenge in high pressure DAC studies. In DAC experiments, there are two commonly used methods to heat samples *in situ*: resistive and laser heating. Resistive heating techniques have the advantage of homogeneously heating the apparatus, therefore providing accurate information on the physical properties of the thermally equilibrated sample. The most commonly used method to measure temperature is through the use of a thermocouple placed near the sample chamber, in direct contact with the diamond anvil and mechanically held in place by the gasket. However, during high temperature experiments, it is impossible to know whether the sample and thermocouple are both at the same temperature during the heating/cooling cycle.¹⁷ In the case of laser heating experiments, the heating is highly localized and temperature is estimated from the black body radiation emitted from the "hot spot," which itself has its own inherent uncertainties.^{18–20}

The difficulties in measuring temperature are manifested by the reported inconsistencies in the phase diagram of hydrogen. It is now established that the melting temperatures of hydrogen exhibit a turnover in temperature as a function of pressure, but there is still widespread disagreement on the exact P-T conditions of the maximum, with the combined experimental efforts placing it in the region from 800 to 1200 K and pressures between 120 and 140 GPa.^{8,10,21–25} There is also disagreement between the melting conditions above 200 GPa, with two studies providing radically different temperatures at a given pressure.^{9,10} At 250 GPa, Howie *et al.*⁹ suggested melting at 450 K, and Zha *et al.*¹⁰ claimed melting at 600 K (see Figs. S1 and S2). This difference in the assignment is not only related to the ability to accurately measure pressure and temperature, but also with the criteria used to define the phase transition.

The only way to determine temperatures unequivocally, regardless of the heating and diagnostic method, is through direct measurements of the physical properties of the material of interest. In this study, we present and compare a variety of techniques for measuring the temperature of H₂(D₂) in both low and high temperature regimes through features in their Raman spectra. There are already established techniques for measuring temperature from the Raman spectra, such as Stokes to anti-Stokes (S/A) ratio, as well as hot-band analysis. Here, we present another complementary method, through the comparison of the intensities of the intramolecular rotational modes (rotons) of H₂ and D₂. The molecular liquid and solid phase I of H₂ and D₂ are the only molecular systems that exhibit free rotation at low-pressure (< 50 GPa) and to low temperatures (0 K) and with the population of the rotational levels governed both by quantum effects and temperature.²⁶ Therefore, as the intensities of the rotational excitations [rotons, S₀(x)] are directly proportional to the thermal occupancy of rotational energy levels, their relative intensities can be used as an absolute temperature gauge.

II. METHODS AND MATERIALS

A. Experimental details

Research grade (99.9999%) hydrogen and deuterium samples were gas loaded into diamond anvil cells at a pressure of 0.2 GPa. Ultra low-fluorescent diamond anvils, with culet diameters ranging between 300 and 400 μm were used. Re-foil gaskets were used to contain the samples, with gasket chambers ranging between 100 and 200 μm. High-quality Raman spectra were acquired using a custom-built micro-focused Raman system, using a 514 nm laser as the excitation line.

During our heating cycles, we primarily used the DE and vibron to monitor pressure fluctuations, which showed isobaricity on heating at 3 GPa.^{14,15} In addition, pressure was monitored by the fluorescence of a ruby chip placed within the sample chamber.¹¹ The use of ruby fluorescence for pressure calibration requires accurate knowledge of the sample temperature: wrong temperatures could result in lack of isobaricity during the experimental runs.²⁷ We note that the use of the thermocouple temperatures leads to unrealistic, i.e., negative pressures, while the use of the spectroscopically determined temperatures yields consistent pressures.

High-temperature experiments were conducted following a previously reported procedure.^{8,9} A type-K thermocouple was partially clamped between the Re-gasket and the diamond anvil. The good mechanical contact ensures a more robust temperature measurement while ensuring optimum proximity to the sample chamber. Heating was done in two stages; a primary heater, external to the cell assembly heating to 550 K; a secondary internal heater, situated around the diamond anvils, heating to 1000 K. The secondary heater consisted of a Mo-coil heating element driven by a DC power supply on a feedback loop with a high sampling rate proportional-integral-derivative (PID) controller.

Low-temperature experiments were conducted by inserting the high-pressure cell in a continuous flow cryostat, using liquid nitrogen as the cryogen. A Pt-100 thermocouple was placed inside the cell body close to the anvils. The cell was first cooled to liquid nitrogen temperature (~ 80 K) for several hours before collecting data on heating.

In all experiments, the following heating/cooling rates were adopted; in the low temperature experiment, the sample was first cooled down to 80 K and then slowly warmed, +3 K min⁻¹. Heating rates for external and internal heating were +6 K min⁻¹ and +30 K min⁻¹, respectively. The known hydrogen diffusivity into both the gasket and diamond anvils at high temperature results in much faster heating rates.

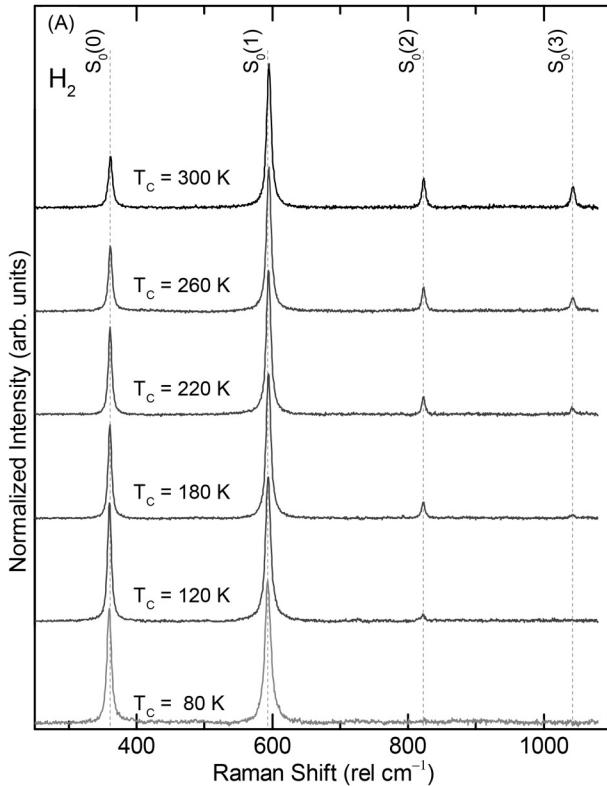
It is important to emphasise that all of the temperature calculations reported in this study are highly susceptible to Raman spectra background subtraction and have to be done with the utmost care to ensure reliable results. The dataset was processed and analyzed using the fitky software package.²⁸ The background and excitations were fitted using a least-squares-based algorithm to polynomial splines and Voigt profiles, respectively.

B. H₂(D₂) temperature measurements using Raman spectroscopy: Rotons as a temperature gauge

Rotational excitations are held by rigid rotor selection rules for Stokes and anti-Stokes, $\Delta J = -2$ (O branch) and $\Delta J = +2$ (S branch), respectively. The quantum mechanical character of H₂(D₂) assures that nuclear spins can be parallel or anti-parallel, resulting in two different species of H₂(D₂), referred to as ortho and para states.²⁶ Both pressure and temperature have an important role in controlling the population of the different ortho/para species^{29,30} and thus controlling the intensity ratio between the ortho/para rotors. To avoid any influence on the proposed roton thermometry method, intensity ratios between ortho/ortho and para/para rotors were only considered.

The intensity of the rotational modes, S₀(x), are directly dependent on the population of their initial rotational level, i.e., J = 0 for S₀. As the populations of the rotational levels are thermally driven by a simple formulism, Eq. (1) can be derived from Maxwell-Boltzmann statistics and incorporated as an additional temperature gauge

$$T_2 = \frac{1}{\frac{k_B}{E_{\text{diff}}} \ln \left(\frac{R_2}{R_1} \right) + \frac{1}{T_1}}, \quad (1)$$



where the roton intensity ratio $R_x = \frac{S_0(J+2)}{S_0(J)}$, the energy difference of the J-transitional $E_{\text{diff}} = E_J - E_{J+2}$, T_x corresponds to temperature, and k_B is the Boltzmann constant. It is possible to directly measure E_{diff} by directly measuring frequency of the rotational modes [hcv_{S₀(J)}]. Additionally, as the ratios R_x are measured from the same species, ortho or para, we negate the impact of ortho-para conversion and its relative contribution. The effects of degeneracy are avoided by using a reference at room temperature.

C. Conventional approaches for Raman thermometry

1. Stokes and anti-Stokes

The Stokes/anti-Stokes relationship as a function of temperature is given in Eq. (2) that includes an additional correction to account for the photon counting of the CCD detector³¹

$$\frac{I_a}{I_s} = \left(\frac{\omega + \Omega_k}{\omega - \Omega_k} \right)^3 \exp \left(\frac{-\hbar \Omega_k}{k_B T} \right), \quad (2)$$

where ω is the excitation wavelength, (I_s) is the Stokes intensity, (I_a) is the anti-Stokes intensity for a given excitation (Ω_k), T is

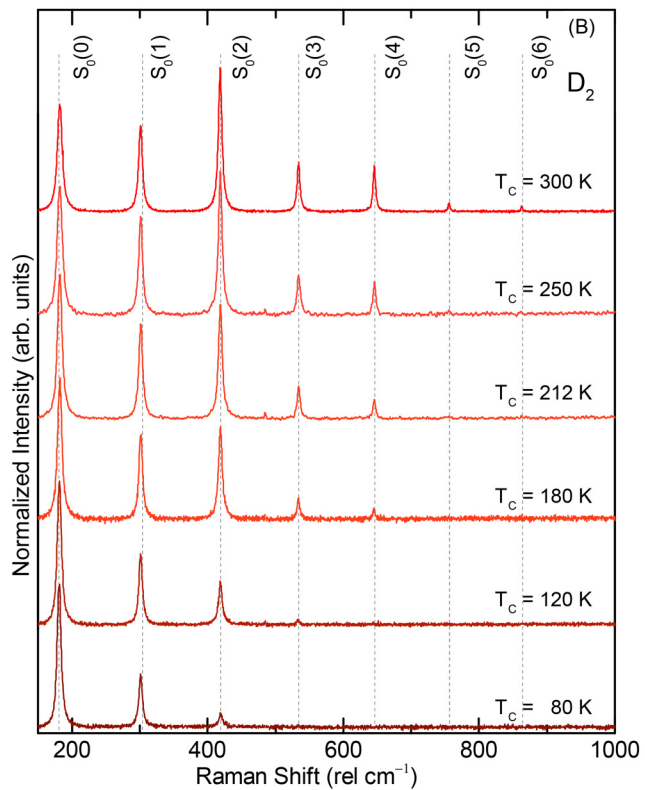


FIG. 1. Representative Raman spectra of hydrogen (a) and deuterium (b) from 80 to 300 K at 3 GPa. The spectra have been normalised so that the total area under each spectrum is equal to 1.

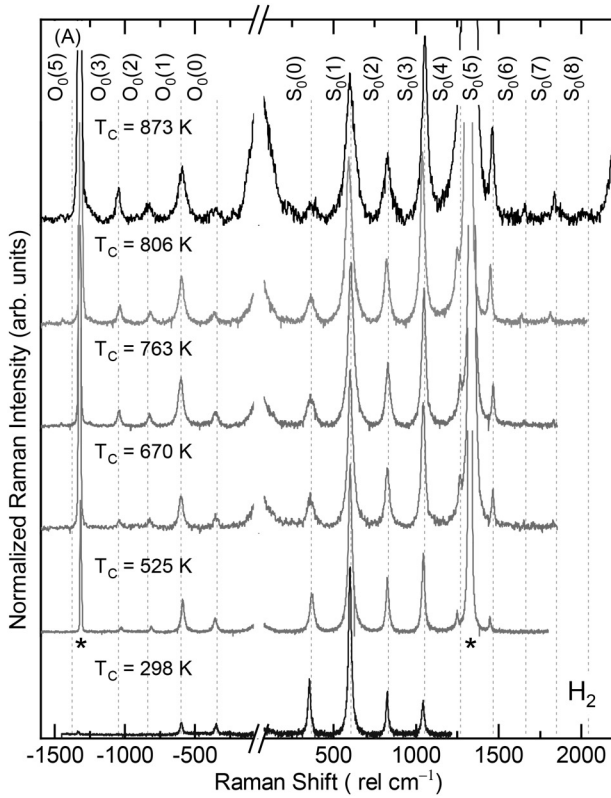
the absolute temperature, and k_B is the Boltzmann constant. The frequencies of the rotational modes of H_2 and D_2 are temperature independent, as shown in Figs. S3 and S4. Thus, to calculate temperatures, we can use Eq. (3), using the S/A intensity ratios $\left[\ln\left(\frac{I_a}{I_s}\right)_R \right]$ at room temperature (T_R) as a reference. This method has been described and adopted in previous studies,³²

$$T_2 = T_R \frac{\ln\left(\frac{I_a}{I_s}\right)_R}{\ln\left(\frac{I_a}{I_s}\right)_1} \quad (3)$$

2. Vibrational hot-bands

At sufficiently high temperatures, additional vibrational modes appear due to the significant population of excited vibrational levels, Q_2 .^{26,33,34} Thus, the sample temperatures can be evaluated by measuring the intensity ratio between fundamental and excited vibrational levels $\frac{I_n}{I_{n+1}}$ and using Eq. (4)³⁴

$$I_{n,n+1} \sim (n+1) \left(\frac{-\hbar\Omega_k}{k_B T} \right), \quad (4)$$



where n is the vibrational quantum number, Ω_k is the Raman frequency of the hot-band (Q_2), T is the absolute temperature, and k_B is the Boltzmann constant.

III. RESULTS AND DISCUSSION

The intensity distribution of the rotational modes in H_2 and D_2 as a function of temperature at 3 GPa is shown in Figs. 1 and 2. As the temperature is lowered, the population of the rotational levels at higher energy decreases, and the rotons with lower energy become the most intense (Fig. 1). For instance, at 120 K, the hydrogen $S_0(2)$ and $S_0(3)$ modes become undetectable. As the rotational modes in deuterium are shifted to lower energies compared with hydrogen (due to the mass difference), the $S_0(2)$ mode is still resolvable at 80 K (see also Figs. S5 and S6).

With increasing temperature (Fig. 2), higher energy rotational levels become accessible, manifested in a redistribution of the roton intensities. The higher energy levels become increasingly populated, while the lower energy levels depopulate. For instance, at 870 K, nine Stokes rotational levels are observable in the H_2 spectrum, while at

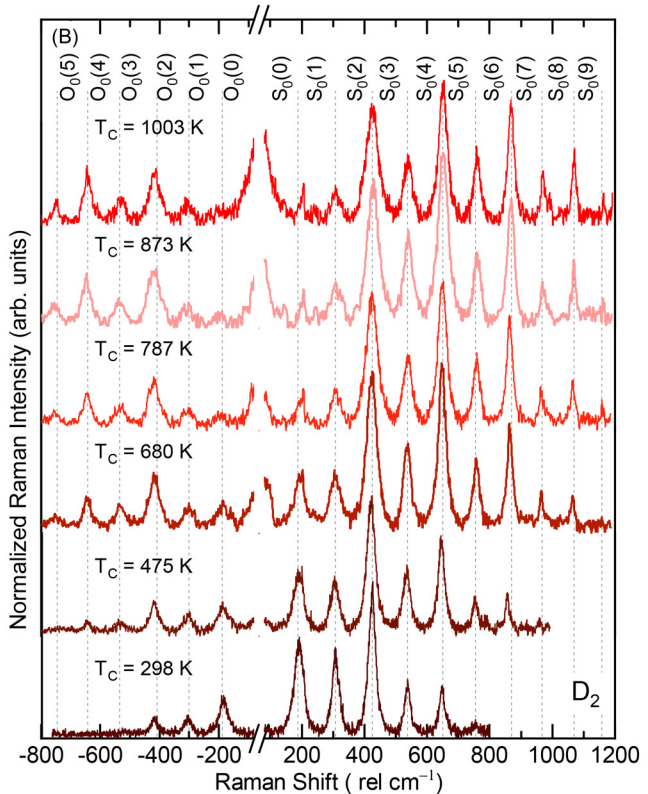


FIG. 2. Representative Raman spectra of hydrogen (a) and deuterium (b) from 298 K to 873/1003 K at 3 GPa. Hydrogen spectra have been normalised to the Stokes $S_0(1)$ mode and the deuterium spectra to the Stokes $S_0(2)$ mode. T_c corresponds to the temperature provided by the thermocouple. The T_{2g} mode of diamond is indicated by an asterisk.

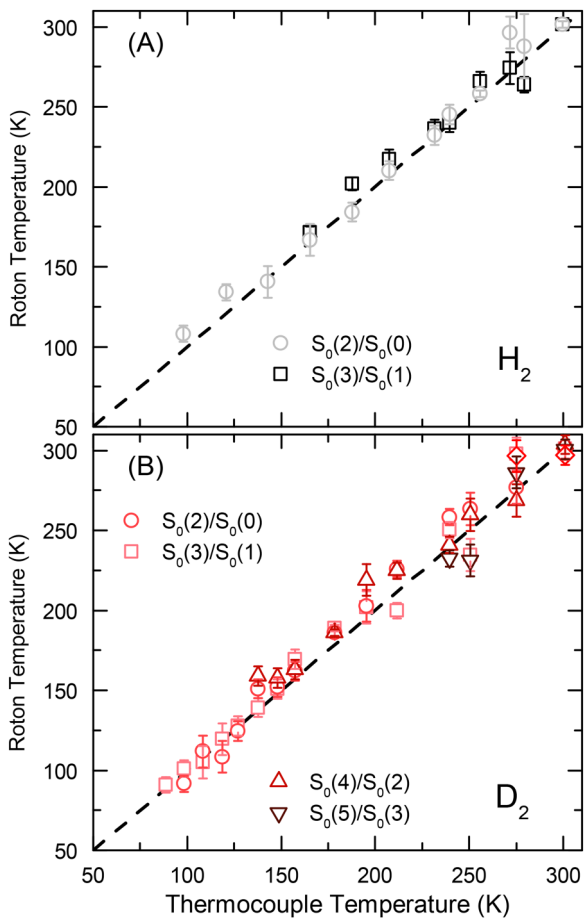


FIG. 3. Temperatures derived from ratios of $S_0(x)$ modes, via Eq. (1) and plotted against thermocouple temperature. Low temperature experiments on hydrogen (a) and deuterium (b) at 3 GPa. Error bars for roton temperatures assume a 5% error on peak fits to the $S_0(x)$ modes. The dashed line indicates where the temperature evaluated from the rotors is equal to the temperature readout from the thermocouple.

least ten are resolvable in D₂; however, the intensity of the S₀(0) roton is close to zero for both isotopes (see also Figs. S7 and S8). Moreover, by increasing the temperature, the excitations in the anti-Stokes region become significantly enhanced and higher anti-Stokes levels (O-) are observed.

As a result of the repopulation and redistribution of roton intensities, the signal-to-noise ratio decreases at higher temperatures. This requires care when measuring, and appropriate spectral collection times, to ensure that all parameters defining the rotational modes can be obtained from their fittings with minimal error. Interestingly, due to the increased collisions between molecules, rotational modes broaden with increasing temperature (Figs. S9 and S10), but their spectral position remains unperturbed (Figs. S3 and S4).

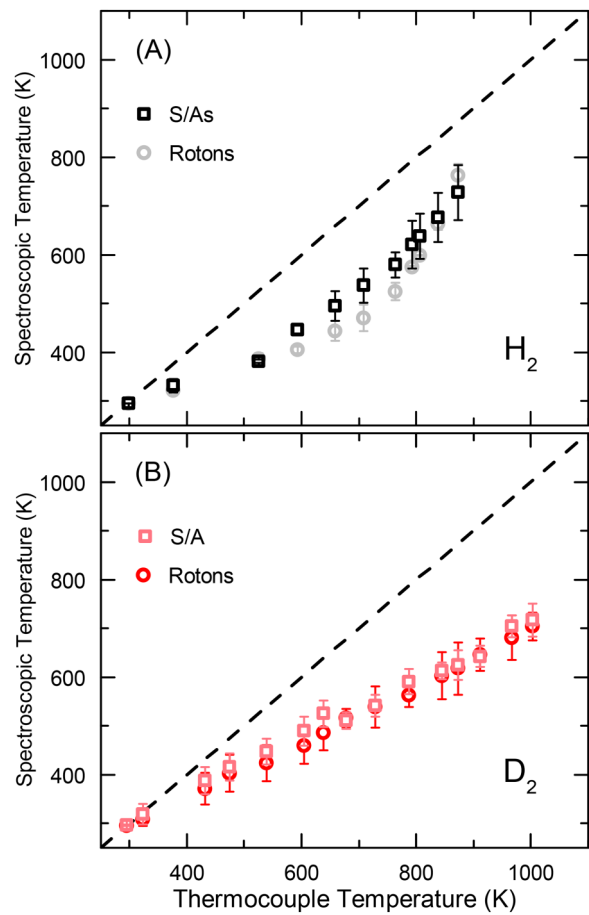


FIG. 4. Temperature derived from ratios of $S_0(x)$ modes via Eq. (1) for Stokes/anti-Stokes (S/A) via Eq. (3), plotted against thermocouple temperature. Resistive-heated hydrogen (a) and deuterium (b) at 3 GPa. Error bars for roton temperatures assume a 5% error on peak fits to the $S_0(x)$ modes. The dashed line indicates where the temperature evaluated from the rotors is equal to the thermocouple readout.

A. Roton analysis at low temperature

Low-temperature experiments provide a good test to validate the use of roton thermometry as the cryostat assembly ensures that both the thermocouple and the sample reach thermal equilibrium before the Raman spectrum is collected. On cooling H₂ and D₂ from 300 K to 80 K at 3 GPa, we see a significant reduction in the intensity ratios of both para [S₀(2)/S₀(0)] and ortho [S₀(3)/S₀(1)] species as a function of thermocouple temperature (see Figs. S11 and S12). However, from these intensity ratios, we can independently calculate the temperature of the sample directly by applying Eq. (1). The resulting roton calculated temperatures are in excellent agreement with the thermocouple temperatures. Figure 3 shows the calculated temperature from the roton analysis versus the thermocouple

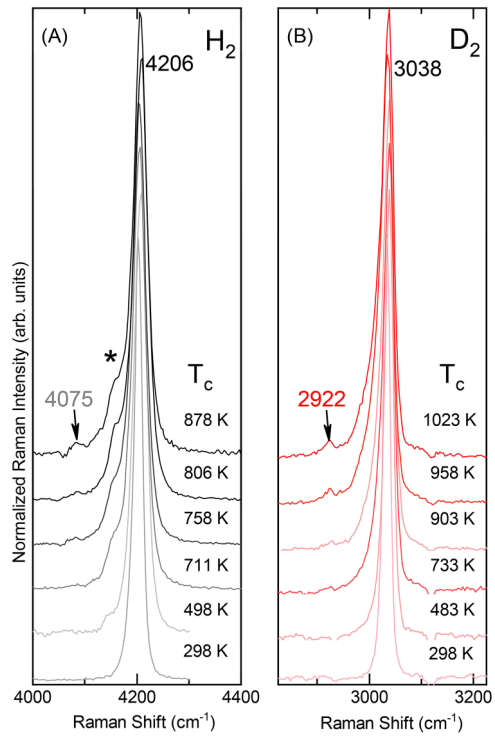


FIG. 5. Normalized vibrational Raman spectra of hydrogen (a) and deuterium (b) at 3 GPa and temperatures up to 1023 K. The Raman frequency of the hotbands (marked with an arrow) is in good agreement with Refs. 26 and 33. The asterisk in (a) indicates the rotational + vibrational band ($Q_1 + S_0$).

temperature, which follows a linear trend, with R-square above 0.985.

This agreement demonstrates that the roton analysis can be used as an accurate temperature gauge. This may be a useful method in low temperature optical measurements, where the laser exposure may lead to sample temperature increases that would not be able to be detected by thermocouple methods. However, the method does have its limitations at low temperatures. The rapid depopulation of the higher order rotational levels (and thus intensities) with decreasing thermal energy eventually leads to only one resolvable rotational band (para in the case of hydrogen and ortho in the case of deuterium). Therefore, it becomes increasingly difficult to obtain a ratio below 120 K for hydrogen and 50 K for deuterium. Thus, the use of roton thermometry allows one to confirm that thermocouple is providing temperatures in agreement with the real temperature of the sample.

B. Roton analysis in resistive heating experiments

With roton thermometry being successfully validated at low temperature, we can implement this method at high temperatures and compare with other thermometry techniques. For both H_2 and D_2 , we have calculated the temperature

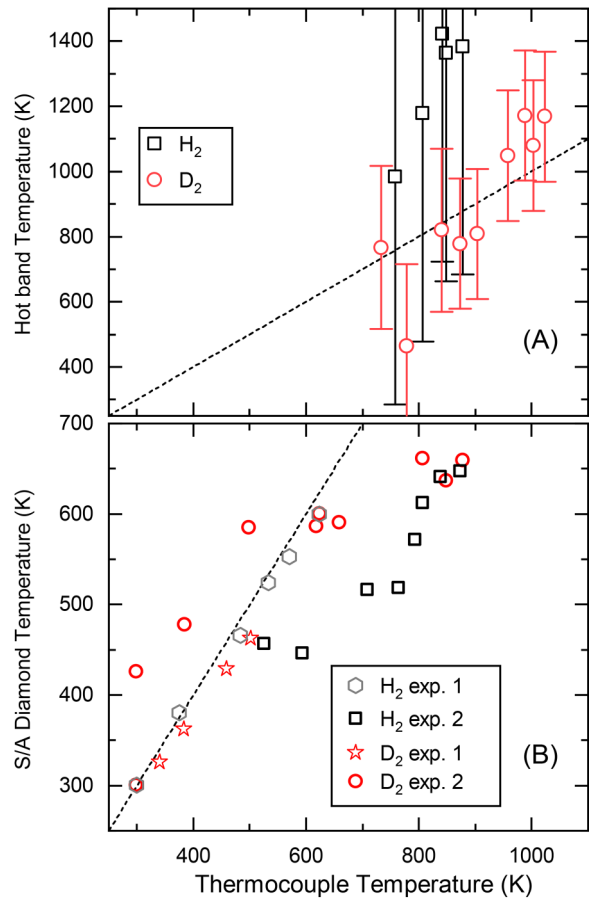


FIG. 6. (a) Vibrational hot band temperature vs. thermocouple temperature for H_2 and D_2 at 3 GPa. (b) Diamond S/A calculated temperature vs. thermocouple temperature for H_2 and D_2 at 3 GPa. The dashed line indicates where the calculated temperature would equal the thermocouple temperature.

through both roton and S/A analysis, via Eqs. (1) and (3), respectively. Figure 4 shows the calculated temperatures plotted as a function of thermocouple temperature for both isotopes (see Figs. S13–S16 for a full dataset). The roton analysis temperatures plotted in this figure are averaged from all the calculated temperatures from each ratio contribution (see Figs. S17 and S18 for individual temperature contributions). We can see that there is an excellent agreement between the temperatures obtained from S/A and roton analysis. However, unlike in the low temperature experiments, there is a clear discrepancy between thermocouple readings and spectroscopically determined temperatures in the resistive heating experiments. There is a relatively good agreement between the temperatures below 400 K but increasingly deviate with temperatures above this.

As described above, resistive heating DAC experiments often use a two-stage setup. Initially, an external resistive heater around the DAC body is used, which results in the DAC

assembly and sample reaching thermal equilibrium. At temperatures above 550 K, a second internal resistive heater is used that is placed around the gasket. This secondary heater provides highly localized heating to the gasket, resulting in extreme thermal gradients. Therefore, the positioning of the thermocouple relative to the sample and the second heater becomes highly important and could provide erroneous thermocouple readings. Such factors could explain the increasing difference between thermocouple and spectroscopic temperatures as temperature is raised. It is impossible to know during a heating experiment both the positioning and integrity of the thermocouple, and our results show that if applicable, spectroscopic thermometries provide a reliable alternative.

The use of the rotational modes as a thermometric tool can be extremely useful when the S/A method is unavailable. However, this method has an important limitation due to the requirement of well defined rotons. It is known that pressure induces the broadening of the rotors in phase I of H₂(D₂).³⁵ Therefore, this rotational thermometry method can only be utilized up to the pressures at which the rotors can be well resolved.

C. Comparison with other thermometry techniques

In Fig. 5, we present the Raman spectra in the vibron region measured during the resistive heating experiments of H₂ and D₂ at 3 GPa. With increasing temperature, the rotational-vibrational band [S₀(x) + Q₁] becomes resolvable as it broadens and separates from the fundamental vibron, (see Figs. S19 and S20 for the Raman shift and an FWHM analysis). At temperatures between 600 and 700 K, the thermal energy is high enough to populate the vibrational excited level and observe the Raman band Q₂. Through Eq. (4), and using the intensity ratios between the fundamental and hot vibron, (Q₁ and Q₂), we have estimated temperatures shown in Fig. 6(a). The low intensity of the hot-band results in significant errors being introduced in temperature estimation (± 200 K for D₂ and ± 600 K for H₂). Since the deuterium vibron has lower energy (3000 cm⁻¹) than hydrogen (4000 cm⁻¹), lower temperatures are required to populate the hot-bands, which explain the lower error observed for the D₂ temperature calculations. The results presented in Fig. 6(a) show that hot-bands cannot be relied upon for thermometry in this temperature regime and overestimate compared with the temperatures obtained through S/A and roton analysis. Another method that could be used to determine temperature is through the Stokes/anti-Stokes intensity ratio of the T_{2g} mode of the diamond anvil. Given the frequency of this mode (1332 cm⁻¹), the anti-Stokes scattering is comparatively weaker compared to the rotational modes of H₂ (D₂), giving poor signal to noise ratio in the 300 K reference spectra. We have calculated the temperatures for several experimental runs using this method and the results are represented in Fig. 6(b). Considering the best spacial resolution, which is able to confocally resolve micrometric samples, thermal gradients within the anvils still yield significant errors in the temperature determination using the S/A method.

IV. CONCLUSIONS

The method of using the intensity ratios of the rotational modes of H₂(D₂) to determine temperature provides a complementary approach to S/A, especially below 1000 K where direct hot-band analysis cannot be performed. The method does have limitations to P-T conditions at which H₂(D₂) can freely rotate presenting well defined rotational modes. Due to the depopulation of rotational levels at low temperatures, the method is also limited to temperatures above 120 K for hydrogen and 50 K for deuterium. However, at high temperature, the use of spectroscopic thermometry becomes increasingly important. By comparison between different experimental resistive heating runs of H₂ and D₂ at 3 GPa, we have demonstrated that thermocouple temperatures do not match those dictated by thermometry which represent the physical properties of the sample.

SUPPLEMENTARY MATERIAL

The supplementary material contains a comparison of the H₂ vibron Raman shift and FWHM on resistive heating at 250 GPa of Refs. 36 and 10. It also shows the Raman spectra as a function of temperature of H₂(D₂) at 3 GPa for low and high temperature experiments. Detailed analysis of the H₂(D₂) Raman shift and FWHM as a function of temperature is also presented for both rotors and vibron. Moreover, temperature obtained through the rotational and S/A approaches are shown for each individual roton.

ACKNOWLEDGMENTS

We would like to thank Dr. A. Coleman, Peter Cooke, and Professor G. Ackland for helpful discussions. M.P.-A. acknowledges the support of the European Research Council (ERC) Grant Hecate Reference No. 695527. Funding has been provided by the respective Chinese 1000 Talent Award grants of both P.D.-S. and R.T.H. X.-D.L. acknowledges the support of the National Science Foundation of China (NSFC) (Grant No. 11874361).

REFERENCES

- ¹S. Scandolo, *Proc. Natl. Acad. Sci. U.S.A.* **100**, 3051 (2003).
- ²S. A. Bonev, E. Schwegler, T. Ogitsu, and G. Galli, *Nature* **431**, 669 (2004).
- ³T. Guillot, *Annu. Rev. Earth Planet. Sci.* **33**, 493 (2005).
- ⁴D. Saumon, G. Chabrier, D. J. Wagner, and X. Xie, *High Press. Res.* **16**, 331 (2000).
- ⁵M. I. Eremets and I. A. Troyan, *Nat. Mater.* **10**, 927 (2011).
- ⁶R. T. Howie, C. L. Guillaume, T. Scheler, A. F. Goncharov, and E. Gregoryanz, *Phys. Rev. Lett.* **108**, 1 (2012).
- ⁷P. Dalladay-Simpson, R. T. Howie, and E. Gregoryanz, *Nature* **529**, 63 (2016).
- ⁸E. Gregoryanz, A. F. Goncharov, K. Matsuishi, H. kwang Mao, and R. J. Hemley, *Phys. Rev. Lett.* **90**, 175701 (2003).
- ⁹R. T. Howie, P. Dalladay-Simpson, and E. Gregoryanz, *Nat. Mater.* **14**, 495 (2015).
- ¹⁰C. S. Zha, H. Liu, J. S. Tse, and R. J. Hemley, *Phys. Rev. Lett.* **119**, 50 (2017).
- ¹¹H. K. Mao, P. M. Bell, and R. J. Hemley, *Phys. Rev. Lett.* **55**, 99 (1985).
- ¹²K. Takemura and A. Dewaele, *Phys. Rev. B* **78**, 104119 (2008).
- ¹³Y. Akahama and H. Kawamura, *J. Appl. Phys.* **96**, 3748 (2004).

- ¹⁴Y. Akahama and H. Kawamura, *J. Phys. Conf. Ser.* **215**, 012195 (2010).
- ¹⁵R. T. Howie, E. Gregoryanz, and A. F. Goncharov, *J. Appl. Phys.* **114**, 073505 (2013).
- ¹⁶X. D. Liu, R. T. Howie, H. C. Zhang, X. J. Chen, and E. Gregoryanz, *Phys. Rev. Lett.* **119**, 065301 (2017).
- ¹⁷M. Santoro, E. Gregoryanz, H.-k. Mao, and R.-J. Hemley, *Phys. Rev. Lett.* **93**, 265701 (2004).
- ¹⁸R. Boehler, *Hyperfine Interact.* **128**, 307 (2000).
- ¹⁹F. Lin, M. Santoro, V. V. Struzhkin, H.-K. Mao, and R. J. Hemley, *Rev. Sci. Inst.* **75**, 3302 (2004).
- ²⁰M. Santoro, J.-F. Lin, V. V. Struzhkin, H.-k. Mao, and R. J. Hemley, "In situ Raman spectroscopy with laser-heated diamond anvil cells," in *Advances in High-Pressure Technology for Geophysical Applications* (Elsevier, 2005), Chap. 20, pp. 413–423.
- ²¹S. Deemyad and I. F. Silvera, *Phys. Rev. Lett.* **100**, 155701 (2008).
- ²²F. Datchi and P. Loubeyre, *Phys. Rev. B* **61**, 6535 (2000).
- ²³M. I. Eremets and I. A. Trojan, *JETP Lett.* **89**, 174 (2009).
- ²⁴A. Goncharov, R. J. Hemley, and E. Gregoryanz, *Phys. Rev. Lett.* **102**, 185502 (2009).
- ²⁵N. Subramanian, A. F. Goncharov, V. V. Struzhkin, M. Somayazulu, and R. J. Hemley, *Proc. Natl. Acad. Sci. U.S.A.* **108**, 6014 (2011).
- ²⁶J. Van Kranendonk and G. Karl, *Rev. Mod. Phys.* **40**, 531 (1968).
- ²⁷S. Rekhi, L. S. Dubrovinsky, and S. K. Saxena, *High Temp.-High Press.* **31**, 299 (1999).
- ²⁸M. Wojdyr, *J. Appl. Cryst.* **43**, 1126 (2010).
- ²⁹Y. Y. Milenko, R. M. Sibileva, and M. A. Strzhemechny, *J. Low Temp. Phys.* **107**, 77 (1997).
- ³⁰J. H. Eggert, E. Karmon, R. J. Hemley, H.-k. Mao, and A. F. Goncharov, *Proc. Natl. Acad. Sci. U.S.A.* **96**, 12269 (1999).
- ³¹J. J. Gallardo, J. Navas, D. Zorrilla, R. Alcántara, D. Valor, C. Fernández-Lorenzo, and J. Martín-Calleja, *Appl. Spectrosc.* **70**, 1128 (2016).
- ³²M. Oron-Carl and R. Krupke, *Phys. Rev. Lett.* **100**, 127401 (2008).
- ³³W. Kolos and L. Wolniewicz, *J. Chem. Phys.* **49**, 404 (1968).
- ³⁴A. F. Goncharov and J. C. Crowhurst, *Phys. Rev. Lett.* **96**, 055504 (2006).
- ³⁵P. Loubeyre, M. Jean-Louis, and I. F. Silvera, *Phys. Rev. B* **43**, 10191 (1991).
- ³⁶R. T. Howie, P. Dalladay-Simpson, and E. Gregoryanz, *Nat. Mater.* **14**, 495 (2015).